27/28th International Conference
**ENGINEERING MECHANICS 2022**
Milovy, Czech Republic, May 9 –12, 2022
Paper **#112,** pp. 7–14, doi: 10.21495/51-2-7

# WAKE BEHIND A CYLINDER: AN OVERVIEW OF SPATIO-TEMPORAL ASPECTS

**Uruba V.***

**Abstract:** *A circular cylinder in crossflow is subjected to the overview study from the point of view spatial and temporal characteristics. It represents itself a typical engineering problem, appearing in practice frequently in various forms. In fluid mechanics, this case is considered to be a typical canonical case, with relatively simple and straightforward definition, but complex and dynamical flow topology. The typical dynamics is characterized by quasi-periodic behavior called von Kármán – Bénard vortex street with a typical frequency expressed in dimensionless number called Strouhal number. The wake flow structure is considered to be characterized by a single frequency and 2D topology, homogeneous along the cylinder axis, very often. The presented paper concentrates on differences between this commonly accepted model and physical reality. Both temporal and spatial aspects of the flow in the wake behind a cylinder are to be addressed. The turbulent subcritical wake characterized by Reynolds number about 5 thousand will be considered, as this situation is a typical case in mechanical engineering applications.*

**Keywords: Circular cylinder, Wake, Vortex, Dynamics, 3D structure.**

## 1. Introduction

A circular cylinder in crossflow is a typical engineering problem, appearing in practice repeatedly in various forms. In fluid mechanics, this case is considered as a typical canonical case, with relatively simple and straightforward boundary conditions, but complex structure of the flow.

In literature, extensive information resources could be found, starting from dawn of fluid mechanics until now. The first systematic work by von Kármán (1954) followed by overview paper by Roshko (1955), and Williamson (1996) to mention the most cited. Interest of researches is not changing a lot during the history, however the technical means applied in the research, involving both experimental approach and mathematical modelling, develops substantially. Recently we have appropriate means available for addressing even the most complex aspects of the phenomenon. And the flow in the wake of a cylinder highly complex is, indeed. It is highly nonstationary and 3D in the same time. However, some aspects were simplified or even neglected in past for the sake of engineering approach. Neglecting 3D aspects could lead to fully unphysical conclusions, e.g., zero drag, the so called d'Alembert's paradox, which could be resolved only by considering the 3D reality, see, e.g., (Hoffman and Johnson, 2010). Some more ideas could be found, e.g., in (Uruba, 2016).

In the present study we will try to address the phenomenon in its complexity of the true spatio-temporal behavior.

The dynamics is simplified very often to a single-frequency periodical process. The von Kármán vortex street is defined and characterized by the Strouhal frequency. The wake structure along the cylinder is considered to be synchronized, and thus 2D. In reality, this approach could be accepted for the fully laminar case only characterized by a very low Reynolds number (*Re*), bellow 150. For higher *Re* values turbulence is present in the wake, the flow should be a broad-band process with random component and fully 3D topology.

In the case of 2D flow structure precondition accepted, then the Navier-Stokes equation could be resolved relatively easily and the solution exists, it is proven by mathematicians. So, the 2D solution is the admissible

* Prof. Ing. Václav Uruba, CSc.: University of West Bohemia, Faculty of Mechanical Engineering, Department of Power System Engineering, Universitní 8, Plzeň, Czech Republic, uruba@kke.zcu.cz, Institute of Thermomechanics of the CAS, v. v. i., Dolejškova 1402/5, 182 00 Praha 8, Czech Republic, uruba@it.cas.cz,

one, however, there is an open question if it is observable in the physical world. Sometimes yes, and sometimes no. The answer depends on the stability of the chosen solution, which should be evaluated carefully. In general, the 2D solution for very low Reynolds numbers could be stable, then the flow is laminar. For higher *Re* the 2D solution becomes unstable. Then the new turbulent, unsteady and 3D solution becomes the stable one in this situation, and thus appearing in the real physical world. The 2D steady state could survive only very limited time period, then it disappears.

The conclusions are valid not only for circular cylinders, but also for the different cross-sections, e.g., rectangular, the situation is qualitatively similar, see, e.g., (Yanovych et al., 2021).

## 2. Reynolds number effect

The Reynolds number is the key dimensionless parameter, which determinates the wake topology and dynamics. Definition of the *Re* involves inlet fluid velocity $U_i$, cylinder diameter $D$ and fluid kinematic viscosity $\nu$ :

$$Re = \frac{U_i \times D}{\nu} \tag{1}$$

Effect of the *Re* on the wake structure is described in many textbooks. Low *Re* values represent extremely small velocities and the wake vanishes (bellow 5), then the steady wake is developed and attached to the body (bellow 44) and for higher *Re* unsteady wake consists of laminar vortex system. For *Re* above 150 the wake is subjected to a laminar-turbulent transition and thus it becomes more and more turbulent, unsteady and 3D.

## 3. Experimental setup

For the sake of demonstration, we have chosen the circular cylinder with diameter $D = 15$ mm and the incoming velocity $U_i = 5$ m/s. The Reynolds number is thus around 5 thousand. The cylinder is sufficiently long (about 250 mm) to consider the 2D boundary condition. The incoming flow is low turbulent and regular. The details on the used experimental facility could be found, e.g., in (Uruba and Procházka, 2020).

The PIV measuring technique was used in classical and stereo versions. The details are given in numerous publications, see, e.g., (Uruba et al., 2020) or (Uruba and Procházka, 2019). In the experiments, 2 planes of measurement (PoM) are chosen to demonstrate the wake structure qualitatively. The situation is shown in Fig. 1.

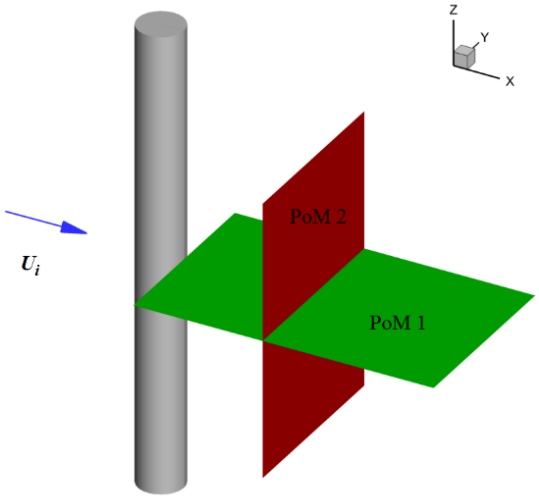


*Fig. 1: The experiment layout, planes of measurement.*

The two PoM are defined in Fig. 1, the PoM 1 is streamwise oriented, perpendicular to the cylinder axis in green and the PoM 2 in red is spanwise oriented, parallel to the cylinder axis in distance 3.83 *D* downstream and perpendicular to the flow in the same time.

The Particle Image Velocimetry (PIV) method was applied, in PoM 1 only in-plane velocity components, while in PoM 2 all 3 velocity components were evaluated. The records consist of 4000 measurements performed with frequency 2 kHz. More details on the measuring technique are, e.g., in (Uruba and Procházka, 2019).

## 4. Results

The results are to be presented in dimensionless form. The space dimensions are shown in multiples of the cylinder diameter $D$, velocities in multiples of the incoming velocity $U_i$.

The frequency $f$ is shown in terms of Strouhal number $Sr$:

$$Sr = \frac{f \times D}{U_i} \tag{2}$$

Time-mean statistics and dynamical patterns in time and space are to be presented first, then dynamical aspects are to be addressed.

### 4.1. Mean flow structure

The time-averaging was performed over acquired instantaneous velocity fields in both PoMs.

First, the streamwise PoM 1 is to be shown in Fig. 2

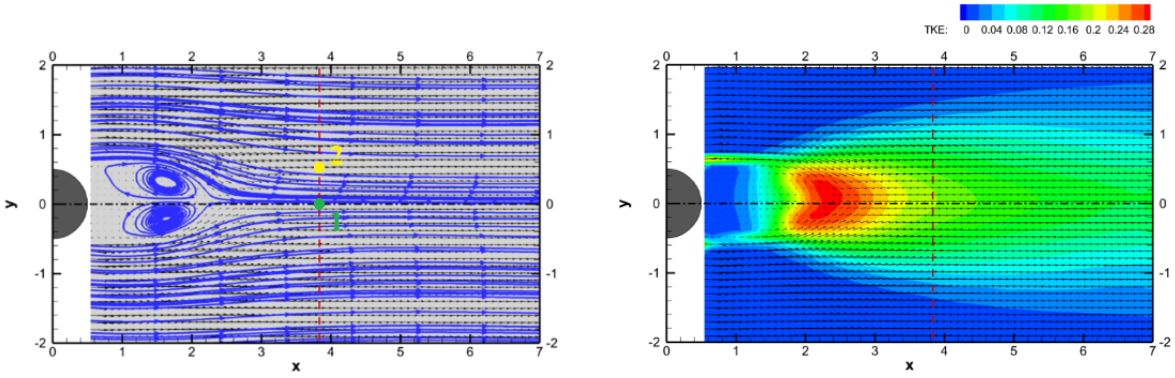


(a) (b)

*Fig. 2: Mean velocity field and TKE in the PoM 1.*

The mean velocity field in the streamwise PoM 1 is in Fig. 2(a), the vector lines (in blue) are shown for clarity. Two vortices dominated the near-wake with a well-defined back-flow region. The dynamical activity is characterized by the Turbulent Kinetic Energy (TKE) distribution in Fig. 2(b). The size of the effective wake is evident and in accordance with the alternative methods applied, see (Duda et al., 2021). Maximal dynamical activity is concentrated in the near-wake, about 2.5 $D$ in the streamwise direction. The red dashed line at position $x$ = 3.83 indicates the intersection with the PoM 2.

In Fig. 3, there are mean results for the spanwise PoM 2, the distribution of streamwise velocity component $U$ in figure (a) and TKE in figure (b). The black dashed lines in positions $y$ = +-0.5 represent the cylinder silhouette. The mean velocity components in $y$ and $z$ directions are negligible in comparison with the $U$ velocity component in $x$ direction.

It is clear that the mean characteristics distributions, both $U$ and TKE, are almost perfectly 2D, varying along the $z$ axis insignificantly.

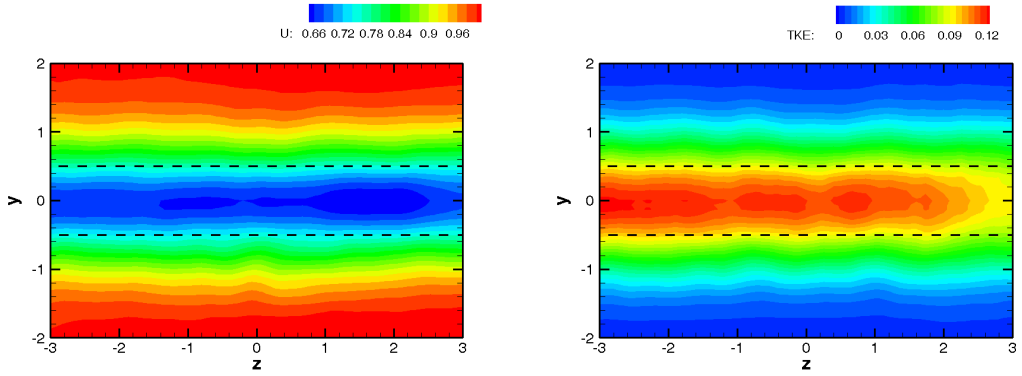


(a) (b)

*Fig. 3: Mean streamwise velocity and TKE in the PoM 2.*

## 5. Dynamics of the wake – temporal aspects

For the analysis, the time-mean field is subtracted, only fluctuations are analyzed bellow.

The spectra of velocity signals in position $x = 3.83$ are to be shown. First the spectra of fluctuations of velocity components acquired at point 1 on the centerline $y = 0$ and then at position $y = 0.5$, point 2. In Fig. 2(a), positions of the two points 1 (green) and 2 (yellow) are shown.

The spectra are to be plotted in log-log coordinates, dimensionless frequency *Sr* and the energy power spectrum is shown in arbitrary units. The dashed lines are at $Sr = 0.21$, 0.42 and 0.63 denoting the 1st, 2nd and 3rd harmonics of the shedding frequency, respectively. The spectra for point 1 are in Fig. 4.

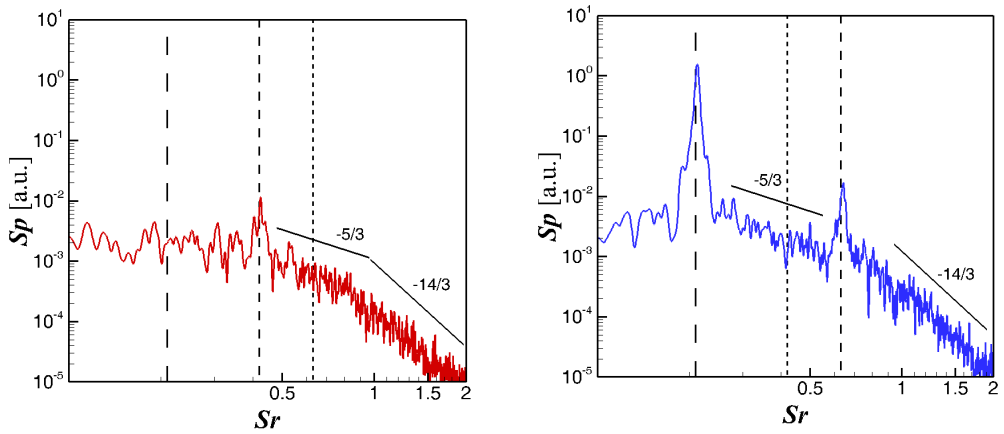


(a) (b)

*Fig. 4: Spectra of streamwise (a) and spanwise (b) velocity components in the point 1 (3.83;0;0).*

The well-developed turbulence is characterized by the spectrum with slope -5/3. The steeper slope, -3 or even -14/3, indicates the presence of the inverse enstrophy cascade appearing in 2D turbulence. This theory is known as the "KLB 2-D turbulence theory" (Kraichnan, Leith and Batchelor) see, e.g., (Garcia et al., 2019). The energy is entering the system somewhere close to the 3rd harmonic $Sr = 0.6$, between the -5/3 and -3 (-14/3) slope regions, and the energy cascade with slope -14/3 or -3 is going towards the higher *Sr*, while the enstrophy cascade with the spectra slope -5/3 is approaching $Sr = 0.2$.

In the 2-D limit, no 3-D dissipative structures are present and, because of the lack of a dissipation mechanism, the turbulent vortical structures can only merge by the enstrophy cascade mechanism.

For the axis position, y = 0, point 1, in the streamwise velocity component spectrum, there is only single and weak peak on the 2nd harmonics, while the spanwise velocity component spectrum shows 2 peaks, on 1st and 3rd harmonics, respectively.

The spectra for the extra-axis point 2 are substantially different, see Fig. 5.

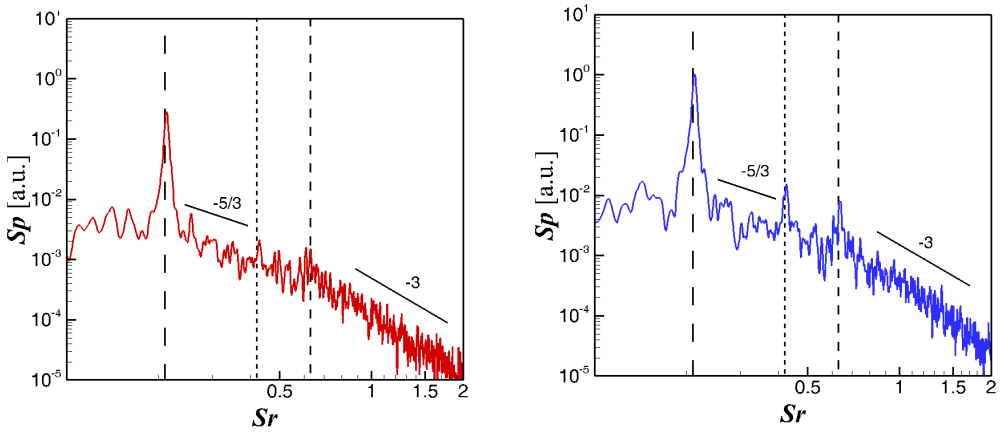


*Fig. 5: Spectra of streamwise (a) and spanwise (b) velocity components in the point 2 (3.83;0;0.5).*

There is a strong peak at the Strouhal frequency for both velocity components, moreover, the higher harmonics are present, but weak. So, the streamwise velocity component measurement on the axis to detect the Strouhal frequency is not recommendable at all. More details on velocity spectra analysis could be found in (Uruba et al., 2020) and (Uruba and Prochazka, 2020).

## 6. 3D structure of the wake – spatial aspects

The spatial aspects of dynamical behavior are to be shown next. The topology of typical structures in terms of fluctuation velocity fields are to be presented.

The Oscillation Pattern Decomposition (OPD) method is applied. The OPD method provides series of OPD modes. Each OPD mode is characterized by its topology in complex form (consisting of real and imaginary parts), frequency $f$ and attenuation of the pseudo-periodic (oscillating) behavior. The attenuation or amplitude decay is described by the so-called e-folding time, $\tau_e$, representing the mean time period of the mode amplitude decay by factor "$e$". The other decay characteristic is the dimensionless "periodicity" $p$ which expresses the e-folding time in multiples of periods of the OPD mode defined by its frequency:

$$p = \tau_e \times f \tag{3}$$

The periodicity value could be considered as a measure of "relevance" of a given OPD mode. The frequency will be represented in dimensionless form as Strouhal number $Sr$, see (2). More details on the OPD method could be found in (Uruba, 2012) and (Uruba, 2015).

The dynamics of the velocity field topology in the PoM 1 was subjected to the OPD analysis. In Fig. 6, there is the spectrum of the case, i.e., frequencies in $Sr$ and periodicities $p$ of the individual modes; 17 OPD modes have been evaluated.

The three dominant modes represent themselves the three harmonic components of the vortex shedding process.

The most dominant is the 1st harmonics, topology of the real part is shown in Fig. 7(a) and imaginary in Fig 7(b). It is represented by the train of vortices with positive (red) and negative (blue) vorticity. The imaginary part is similar to the real one, but the vortices are shifted in streamwise $x$ direction by a quarter of period. This means that the OPD mode 1 represents a wave or train of vortices with alternating orientations, moving in the streamwise direction.

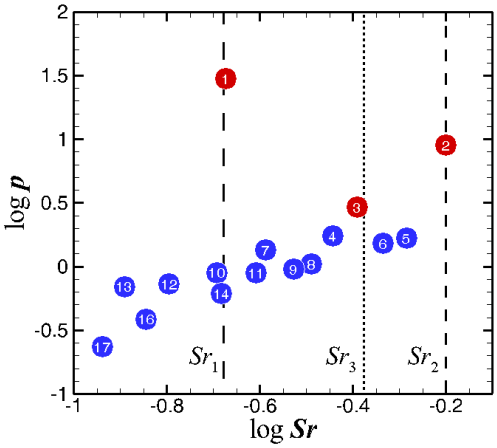


*Fig. 6: OPD spectrum of velocity field in the PoM 1. Shown in log coordinates.*

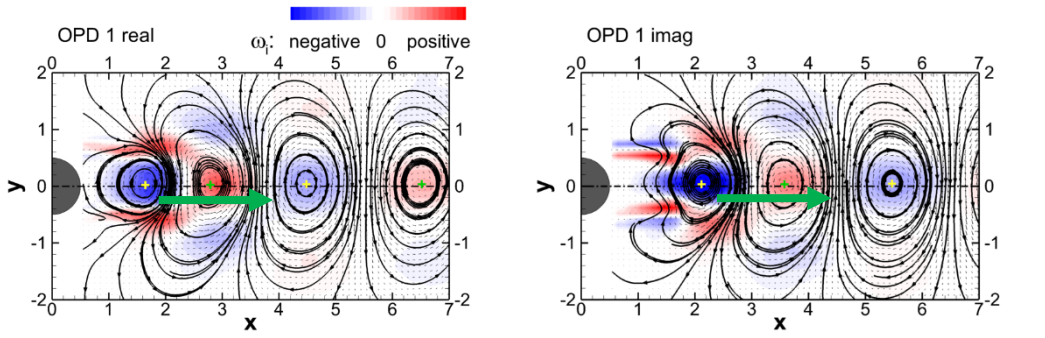


(a) (b)

*Fig. 7: Topology of the 1st OPD mode, PoM 1, real (a) and imaginary (b) parts.*

In Fig. 8(a), there is the real part of the OPD mode 2 with frequency corresponding to the 3rd harmonics of the process, $Sr = 0.63$. The imaginary part (not shown) is again shifted in $x$ direction. The topology is very similar to that of the 1st OPD mode, only the density of vortices is much higher. The OPD mode 3 is depicted in Fig. 8(b), it corresponds to the frequency of the 2nd harmonics. The topology is formed by contra-rotating vortices in a row convected in the streamwise direction.

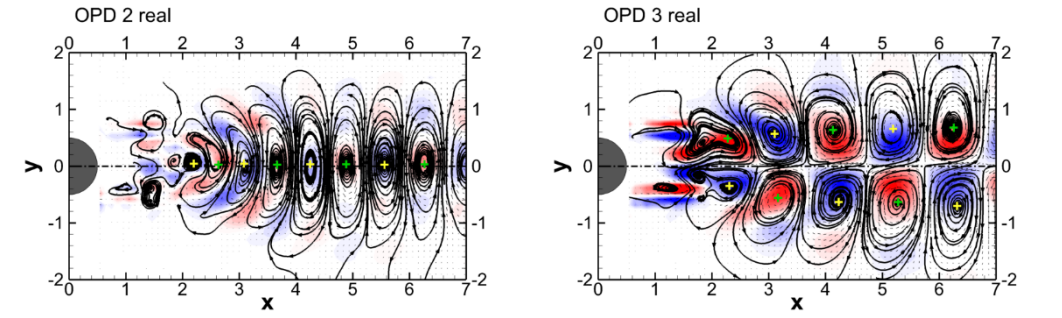


(a) (b)

*Fig. 8: Topologies of real parts OPD modes 2 (a) and 3 (b), PoM 1.*

The convective velocity of the vortex structures is a detected to be a little bellow the incoming flow velocity $U_i$, and it is approximately the same for all 3 OPD modes in question.

The higher order modes consist of system of vortices, but the topology is rather chaotic and there is no clear wave character. More detailed analysis is shown in (Uruba and Prochazka, 2020).

Next, the dynamics in the PoM 2 is to be presented. All three velocity components enter the analysis.

The OPD analysis reviled 8 modes, the dominant modes 1 and 2 are located around the shedding frequency $Sr_1 = 0.21$. The mode 3 is at a little higher frequency and the higher order modes are for much lower frequencies. The OPD spectrum is in Fig. 9.

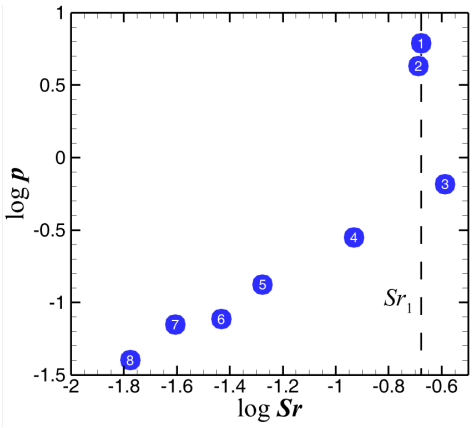


*Fig. 9: OPD spectrum of velocity field in the PoM 2. Shown in log coordinates.*

The topology of the dominant OPD 2, both real and imaginary parts, are shown in Fig. 10. Please note, that the color means here the out-of-plane velocity component $U$, positive in red and negative in blue. There are big velocity strips close to the cylinder silhouette, forming a checkered pattern, the opposite orientation in upper – lower parts and right – left parts, respectively. On the top of that, the in-plane vortex is present, this means that the vortex has its axis in the streamwise direction $x$. Both the vortex and velocity strips are moving from the right to the left-hand-side forming the waves moving along the cylinder axis $z$.

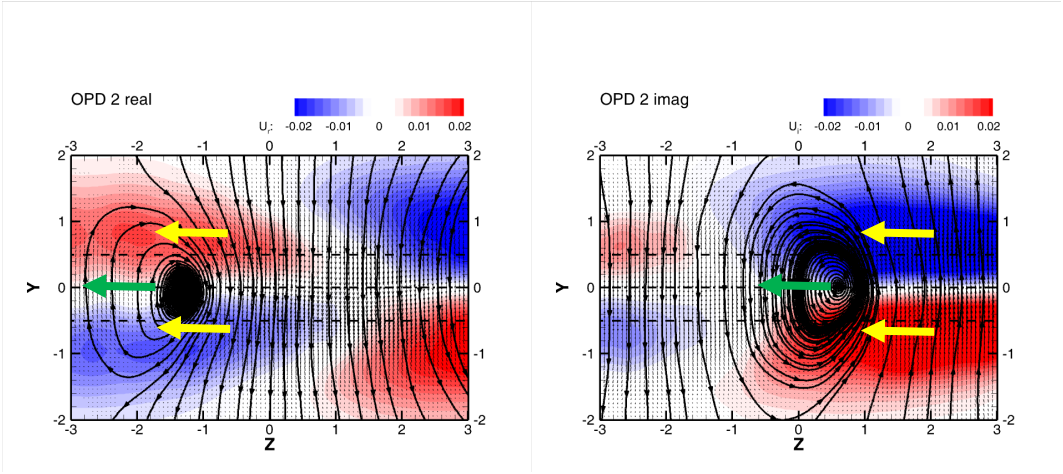


(a) (b)

*Fig. 10: Topology of the 1st OPD mode, PoM 2, real (a) and imaginary (b) parts.*

Examples of the higher order OPD modes of the dynamics in the PoM 2 are shown in Fig. 11, where real parts of modes 5 and 6 are shown, respectively.

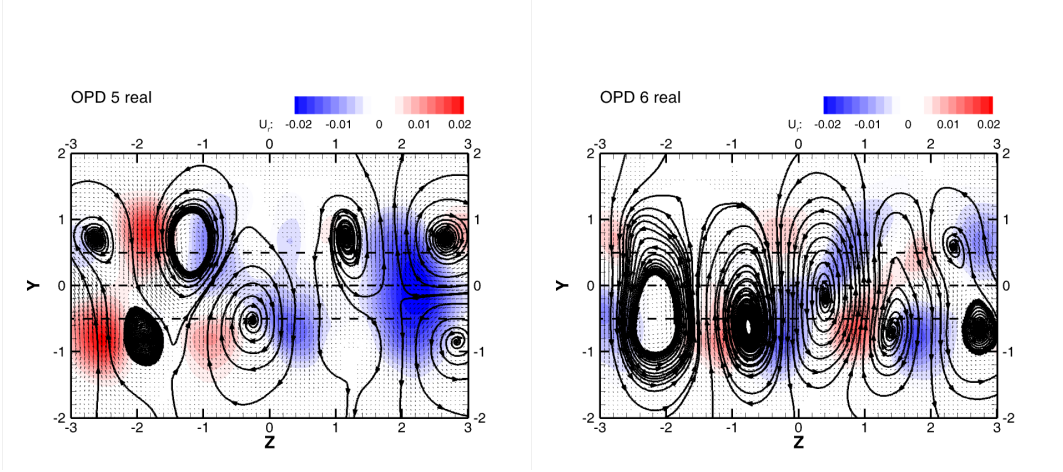


(a) (b)

*Fig. 11: Topologies of real parts OPD modes 5 (a) and 6 (b), PoM 2.*

The higher-order modes topology in the PoM 2 is formed by the system of jets in the positive and negative streamwise direction and the system of vortices with axes oriented in streamwise direction $x$ as well.

The imaginary parts of the modes topologies are similar, however the positions of structures is slightly modified. However, no systematic convection of the structures was detected within the modes dynamics. Frequencies are about $Sr = 0.117$ for the mode 5 and 0.053 for the mode 6, i.e., much lower than the shedding frequency.

## 7. Conclusions

In the paper, the dynamical aspects of the fully turbulent wake behind a circular cylinder in cross-flow, Reynolds number about 5 thousand, are shown on the basis of the experimental research results. This situation is typical for many engineering applications.

The presented results clearly show that the flow in wake is a broad-band dynamical process with 3 dominant frequencies corresponding to 3 harmonics of the vortex shedding process.

The topology of the dynamical structures is highly 3D and could not be modelled properly by a 2D dynamical model. A typical dynamical patterns topology is presented.

## Acknowledgement

The presented matter results from joint research conducted during last year in several institutions together with my coworkers: P. Procházka, V. Skála from the IT ASCR, D. Duda, V. Yanovych, from the UWB and S. Pospíšil, P. Michálek from the ITAM ASCR.

This publication was supported by the project of University of West Bohemia in Pilsen SGS-2022-023.

## References

Duda, D., Uruba, V., and Yanovych, V. (2021) Wake Width: Discussion of Several Methods How to Estimate It by Using Measured Experimental Data, *Energies*, Vol. 14, 4712.

Garcia, B., Weymouth, G., Nguyen, V., and Tutty, O. (2019). Span effect on the turbulence nature of flow past a circular cylinder. *Journal of Fluid Mechanics,* Vol. *878*, 306-323. doi:10.1017/jfm.2019.637

Hoffman, J., and Johnson, C., (2010) Resolution of d'Alembert's paradox, *Journal of Mathematical Fluid Mechanics*, Vol. 12 (3), pp.321-334.

Michálek, P., Pospíšil, S., Procházka, P., and Uruba, V. (2022) Influence of surface roughness on the wake structure of a circular cylinder at Reynolds numbers $5x10^3$ to $12x10^3$, *to be published*.

Roshko, A. (1955) On the development of turbulent wakes from vortex streets. *NACA Rep. 1191*, pp.801-825.

Uruba, V. (2012) Decomposition methods in turbulent research, *EPJ Web of Conferences*, Vol. 25, 01095.

Uruba, V. (2015) Near Wake Dynamics around a Vibrating Airfoil by Means of PIV and Oscillation Pattern Decomposition at Reynolds Number of 65 000, *Journal of Fluids and Structures*, 55, pp. 372-383.

Uruba, V. (2016) On 3D instability of wake behind a cylinder, *AIP Conference Proceedings*, Vol. 1745, 020062.

Uruba, V., and Prochazka ,P., (2020) POD Spectrum of the Wake behind a Circular Cylinder, *MATEC Web of Conferences,* Vol. 328, 05006.

Uruba, V., and Procházka, P. (2019) The Reynolds number effect on dynamics of the wake behind a circular cylinder, *AIP Conference Proceedings*, Vol. 2189, 020023.

Uruba, V., and Prochazka, P. (2020) On Harmonic Contents of the Wake behind a Circular Cylinder, In: Fuis, V., ed., *Engineering Mechanics 2020*, Brno University of Technology, Brno, pp.500-503.

Uruba, V., Procházka, P., and Skála, V. (2020) On the 3D Dynamics of the Wake Behind a Circular Cylinder, In: Šimurda, D. and Bodnár, T., eds., *Proceedings Topical Problems of Fluid Mechanics 2020*, Prague, pp. 240-248.

von Kármán, T. (1954) *Aerodynamics*. Columbus: McGraw-Hill.

Williamson, C.H.K. (1996) Vortex Dynamics in the Cylinder Wake, *Annual Review of Fluid Mechanics,* Vol. 28, pp. 477-539.

Yanovych, V., Duda, D., and Uruba, V. (2021) Structure turbulent flow behind a square cylinder with an angle of incidence, *European Journal of Mechanics, B/Fluids*, Vol. 85, pp. 110-123.